Quantitative GPR inspection of quasi-homogeneous ground layers

Victor Yavna, *Zelimkhan* Khakiev, *Georgy* Lazorenko*, *Anton* Kasprzhitskii *and Sergey* Sulavko

Rostov State Transport University, Chair of Physics, Narodnogo Opolcheniya Sq., Rostov-on-Don, 344038, Russian Federation

Abstract. This work covers methods of GPR monitoring of constructions that are quasi-homogeneous ground layers. The monitoring methods include the determination of complex dielectric permittivity and moisture of the construction layers of highways and railways. In order to obtain quantitative values of these parameters the GPR method is calibrated via the measurement of these quantities using the resonance method at frequencies close to the central frequency of the microwave radiation used.

1 Introduction

Modern large-scale construction and upgrading of highway and railway nets led to the creation of high-performance diagnostic complexes which include the GPR method [1, 2] as a basic geophysical method for diagnostics of the state of extended quasi-homogeneous construction layers [3, 4].

Today, the progress in the GPR studies allows successful solving of various engineering problems. In particular, in [5-7] authors solve the problems of searching and classifying the cracks in the road pavement. Positioning of cracks and corrosion of the reinforcing bars in concrete structures of bridges is studied in [8, 9]. The GPR method is used to measure dielectric permittivity and conductivity of soils and building materials [10-12]. In addition to dimensioning, the GPR method allows estimating the moisture level of constructional and ground layers since the amount of water is the main factor affecting electromagnetic wave propagation [13]. The presence of water in the ground layers significantly affects their mechanical properties and substantially determines reliability and durability of a construction [14, 15].

Therefore, one of the most popular subjects of the research in the field of GPR application is the estimate of the water content in soils [16-19]. Due to the swelling destruction of engineering communications and road constructional layers in permafrost areas, the GPR method is also of great interest for monitoring the permanently frozen grounds [20, 21]. The above proves the relevance of the researches aimed at developing the methods of obtaining quantitative information on soil's properties from the GPR data.

* Corresponding author: glazorenko@yandex.ru

On the other hand, the dielectric permittivity and electric conductivity of soils and materials can be carried out by direct electric measurements, see, for example, [20, 22]. These methods can be used for calibrating the data obtained from the GPR surveys.

The aim of this work is to develop the method for determining permittivity and moisture of ground layers of highways and railways using the GPR data calibrated via the resonance method of measurement of complex dielectric permittivity.

2 Methods

2.1 Resonance method for measurement of dielectric permittivity and electric conductivity of soils

Determination of complex permittivity of a sample is based on the comparison of the results of direct measurements of the resonance frequency and the Q-factor of a sample with those values obtained by computer simulation at given values of permittivity (ε) and conductivity (σ). The measuring equipment includes: transmission and reflection coefficient meter P2M-04 operating within the frequency range 10 MHz – 4 GHz, computer with specialized software for the experimental data processing, a microwave cavity made of brass (Fig. 1) which includes a container (b) for a sample (c). The container is made of plastic with dielectric permittivity of 2.98.

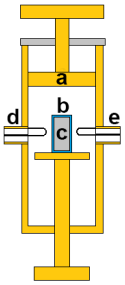

Fig. 1. General view of the microwave cavity: a- resonator, b- plastic container, c- sample, d- port 1, e- port 2.

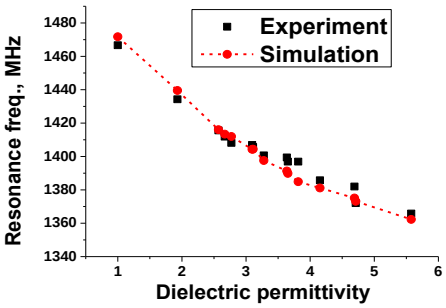

Fig. 2. Dependence of resonance frequency on dielectric permittivity.

Theoretical study of resonant properties of soils is performed by computer simulation of the electric field propagation in the microwave resonator with different materials [23]. The computer model of a microwave cavity is created in the environment CST STUDIO SUITE. For each component of the model (Fig. 1) geometrical dimensions and physical parameters (permittivity and conductivity) were set in accordance with the experimental prototype. The Finite Integration Technique (FIT) using the «Eigenmode Solver» software

block is applied with partitioning of space into discrete hexahedral cells. Calculated and measured resonance frequencies for the reference samples with specified dielectric permittivity were compared to assess the accuracy of the theoretical data. Theoretical and experimental results are given in Figure 2. The accuracy of the computer model and the numerical routine can thus be estimated to be 2%. Upon the increase of the moisture of a soil sample placed in the cavity, the dielectric losses grow. Therefore, besides the real part of the complex dielectric permittivity, the conductivity (σ) is introduced in the computer model as an additional parameter in order to take these losses into account:

$$\sigma = \sigma^* + \sigma_{cm} \tag{1}$$

where σ^* is the conductivity of the sample in the container, and σ_{cm} is the conductivity of the plastic container material ($\sigma_{cm} = 0.92 \cdot 10^{-3}$ S/m). Hereafter, the physical parameters determined by the resonance method are marked with the asterisk (*). The value of σ^* is chosen so that the width of the theoretical resonance curve ($\Delta\omega$) at half maximum coincided with the experimental one. Then

$$\sigma^* = \varepsilon\varepsilon_0\Delta\omega \tag{2}$$

2.2 GPR Method of Measurement the Properties of a Soil Sample

In the case of the monochromatic wave approximation, the absorption coefficient which is determined by both absorption and scattering of electromagnetic radiation (p_e), and the absolute index of refraction (n), according to [24], can be written as:

$$p_e = \frac{\omega}{c}\sqrt{\frac{1}{2}\left\{-\varepsilon + \sqrt{\varepsilon^2 + \frac{\mu_0^2 c^4 \sigma^2}{\omega^2}}\right\}} \tag{3}$$

$$n^2 = \frac{1}{2}\left\{\varepsilon + \sqrt{\varepsilon^2 + \frac{\mu_0^2 c^4 \sigma^2}{\omega^2}}\right\} \tag{4}$$

where (ω) is the cyclic frequency, (c) is the speed of light in vacuum, and (μ_0) is the magnetic permittivity of vacuum.

Since the pulse radiation of a georadar is not monochromatic, we use in our calculations with (1-2) the most probable cyclic frequency (ω). For the AB-1700 antenna with central operating frequency f = 1700 MHz, the cyclic frequency is $\omega = 2\pi f$. Algebraic manipulations with the expressions (3, 4) allow relating the absorption coefficient to the conductivity via the formula

$$\sigma = \frac{2 p_e n}{\mu_0 c} \tag{5}$$

When propagating in medium, the electromagnetic radiation experiences spatial divergence, which can be characterized by the attenuation coefficient (Δp). This effect can be illustrated by the electromagnetic field simulation. The field is produced by the transmitting antenna (Fig. 3) which is placed in the air at some distance from the soil with permittivity (ε).

Computer model for the calculations is developed in the CST Microwave Studio Suite. The bowtie-type antenna element is made of copper with electric conductivity $\sigma = 5.99 \cdot 10^7$ S/m. It is placed into a metallic box which serves for suppression of the reverse lobe of the beam pattern. The design of the bowtie-type antenna also has the external (200 Ohm) and

internal (50 Ohm) active resistors. The antenna is excited by a Gaussian pulse with the central frequency of 1200 MHz and the width at half maximum of 0.6 MHz. These pulse parameters were chosen for the best description of the experimental results. Instant electric field intensity distribution was determined by numerical solution of Maxwell's equations within FIT using the Perfectly Matched Layers (PML) boundary conditions for the computational domain. Calculation results are shown in Figure 3.

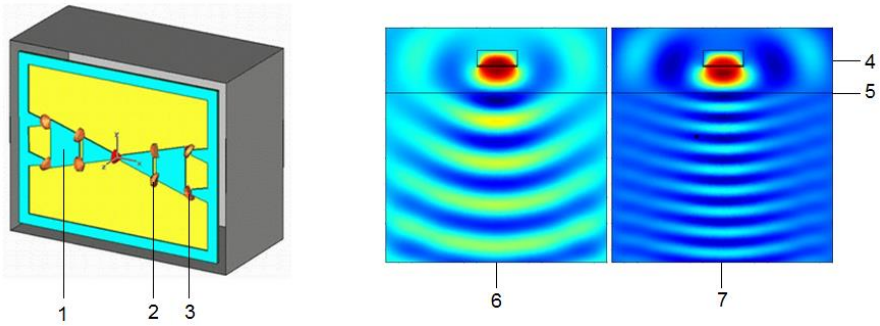

Fig. 3. General view of the computer model of a bowtie-type antenna (1) with internal (2) and external (3) active resistors, and also electric field produced by the antenna unit placed in the air (4). Line (5) shows the boundary of the media with dielectric permittivity $\varepsilon = 2.5$ (6) и $\varepsilon = 10.0$ (7).

The value of attenuation coefficient of electromagnetic radiation during the GPR measurements (p) is determined by the formula:

$$p = \Delta p + p_e \tag{6}$$

A general scheme for determining the attenuation coefficient from the GPR data can be described as follows. Let us denote the trace of the GPR measurements on the depth scale as $F = F(r)$. Further, apply the Hilbert transformation to $F(r)$

$$G = \hat{G}(F(r)) \tag{7}$$

where $r = \sum_i \tau \cdot m_i \cdot c / n_i$, ($c$) is the speed of light in vacuum, index (i) is used to number the discrete points of the trace $F(r)$ during the measurements, is the index of refraction in the corresponding point of the construction. The result of the transformation for an arbitrary two-layered medium is shown in Figure 4.

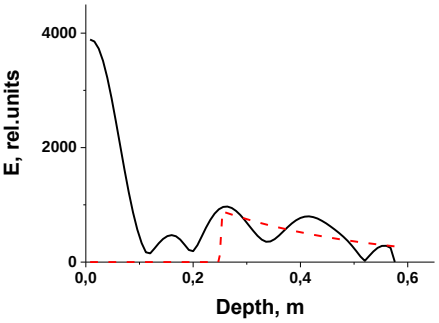

Fig. 4. Approximation of the GPR trace when calculating the attenuation coefficient for the layer.

Assume that some constructional layer is limited by upper and lower boundaries having coordinates (h_1) and (h_2), respectively. In order to determine the attenuation coefficient, let us approximate (7) with

$$G(F(r)) = \hat{G}(F(\mathrm{h}_2)) * e^{-p(h-h_1)} + \hat{G}(F(h_2)) \tag{8}$$

The result of such an approximation is shown in Figure 4 with a dashed line.

2.3 Calibration of the GPR data, method №1

As mentioned above, the resonance method allows measuring the dielectric permittivity (ε^*) and the electric conductivity (σ^*) of a ground sample extracted from a construction layer. Using these values in (4) makes it possible to calculate the absolute index of refraction (n). To calculate the absorption coefficient one can use (3) or (5).

Measurements of the GPR traces of construction layers in their physical state under study allows one to determine the signal attenuation coefficient and then to calculate using (6). Hereafter we suppose that this value changes little when the properties of the construction layers alter. Further on, we determine the positions of upper (m_1) and lower (m_2) boundaries of the construction layers from the GPR traces, and the number of sampling points of the trace on this interval: $\Delta m = m_2 - m_1$.

Absolute refraction index of a layer upon the variation of its moisture without any geometry changes can be obtained from the following equation:

$$n = n^* \left(\frac{\Delta m}{\Delta m^*} \right) \tag{9}$$

Determination of attenuation coefficient of electromagnetic radiation by the GPR method allows calculating the value of absorption coefficient (p_e) by (6) (assuming (Δp) is constant), and (σ) and (ε) by (5) and (4), respectively.

It's obvious that this calibration method can be applied to all the construction layers independently.

2.4 Calibration of the GPR data, method №2

The calibration method described above includes determination of attenuation coefficient via the approximation of the GPR traces. This mathematical routine can be replaced by the analysis of the amplitudes of signals reflected from the boundaries of constructional layers. Consider the results of the GPR surveys in which the georadar antenna unit is placed above the uppermost construction layer of the road bed at certain height. Suppose the chosen height provides separation in time of the direct signal (from transmitter to receiver), and the signal reflected from the upper boundary of the first construction layer. Then the amplitude (E_0) of the signal incident on the road bed can be estimated with the equation:

$$\frac{E}{E_0} = \sqrt{\frac{(n_1^* - n_0)^2 + (\chi_1 - \chi_0)^2}{(n_1^* + n_0)^2 + (\chi_1 + \chi_0)^2}} = A_{0,1}^*, \tag{10}$$

where the indexes «1» and «0» refer to the material of constructional layer and air, respectively. The amplitude of the reflected signal (E) is determined using the GPR data. The following notations are used in (10):

$$\chi_1 = \frac{c}{\omega}(p^*_{e,1} + \Delta p)\,,\quad \chi_0 = \frac{c}{\omega}\Delta p\,, \tag{11}$$

where (Δp) is taken to be equal to the value, defined in the previous section. We use it in the above relations to weaken the effect of the plane wave approximation used in (10). When the physical state of the layers change, one can use (9) to determine the absolute refractive index of the layer number «*i*», and then determine the attenuation coefficient from expression (12), applying it to the layers sequentially, starting from the first:

$$\frac{E_i}{E_0} = \sqrt{\frac{(n_i - n_{i-1})^2 + (\chi_i - \chi_{i-1})^2}{(n_i + n_{i-1})^2 + (\chi_i + \chi_{i-1})^2}} \prod_{k\rangle 0, i-1-k\rangle -1} (1 - A_{i-1-k,i-k})^2 e^{-2\frac{\omega}{c}\chi_{i-k}} \tag{12}$$

3 Results and discussion

Formulas (3-6) and (10, 12), proposed for calculating the physical parameters of structural layers of automobile and railroads, were obtained using the approximation of the normal incidence of plane electromagnetic waves on the interface between media. Except that, Δp is assumed to be constant for different construction layers. The validity of these assumptions when interpreting the GPR data is not evident. Therefore, an estimate of method's inaccuracy is necessary. This estimate was performed in this work by application of the method for determining the values of dielectric permittivity and conductivity of fine river sand samples with different moisture. The sand was placed into a cubic-shape volume with the side of 0.5 m. The antenna unit was placed above the sand surface at the height of 0.15 m. Moisture of the sand used for GPR data calibration was determined as 0.51 %.

Results of calculation are given in Table 1

Table 1. Physical parameters of the sample at the GPR calibration point (W = 0.51%).

	ε^*	$\sigma^* \cdot 10^3$S/m	p^*_e, m^{-1}	p, m^{-1}	$\Delta p^*, m^{-1}$	n^*
Method	Resonance	Resonance	Formula (3,5)	Radargram	Formula (6)	Formula (4)
Value	3.30	3.71	0,38	3.63	3.25	1.82

After changing the humidity of the sand, the positions of the layer boundaries, m_1, m_2, its extent on the georadar trace Δm, and the attenuation coefficient for electromagnetic radiation p were determined by the GPR method.

Calculated values of absolute index of refraction and attenuation/absorption coefficients for the sand samples with different moisture W are given in Table 2.

Table 2. Properties of sand samples with different moisture calculated using calibrated GPR data.

W,%	*Δm*	*n*	p_e+Δp^*	p_e	*σ, S/м*	*ε*	*σ,* S/m	*ε*
Method of determining	Radar-gram	Form. (7)	GPR	Form. (9)	Form. (5)	Form. (4)	Resonance method	Resonance method
0,51	104	1,82*	3,63	0,38	0,0037	2,8	0,0037*	,30*
1,78	126	2,21	4,18	0,93	0,0109	3,8	0,0056	3,46
2,196	139	2,43	4,01	0,76	0,0098	4,8	0,0097	4,54
4,84	157	2,75	4,08	0,83	0,0121	6,2	0,0163	6,63
7,73	184	3,22	4,34	1,09	0,0186	8,8	0,0232	8,57
10,01	204	3,57	4,99	1,74	0,0330	10,7	0,0265	10,56
14,42	252	4,37	6,20	2,95	0,0684	16,4	0,0553	17,14

16,05	255	4,46	6,33	3,08	0,0729	19,1	0,0593	18,35

The accuracy of the parameters obtained by calibrated GPR method is estimated with respect to the resonance measurements (last two columns of Table 2 highlighted with grey). The values of respective errors are illustrated in Figure. 5.

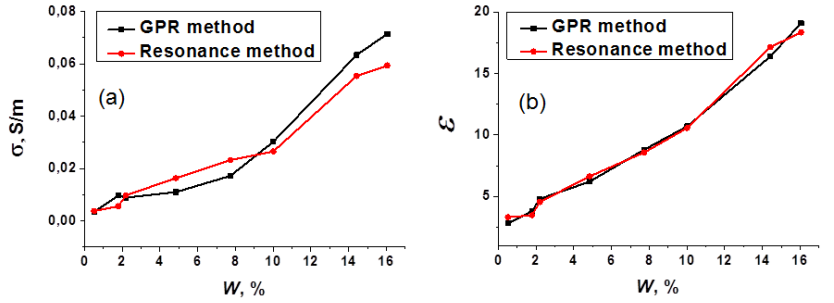

Fig. 5. Electric conductivity (a) and dielectric permittivity (b) of the sand samples with different moisture.

It can be seen that the deviation of permittivity and conductivity obtained with the calibrated-in-single-point GPR method from those obtained with the resonance method, does not exceed 10-15%.

To estimate the possibility of applying formula (12), the amplitude of the signal reflected from the upper boundary of the sand layer is calculated depending on its humidity. Attenuation coefficients given in Table 2 are used in the calculations. Calculations results are referred to the amplitude at moisture W=16.05%; they are shown in Figure 6a.

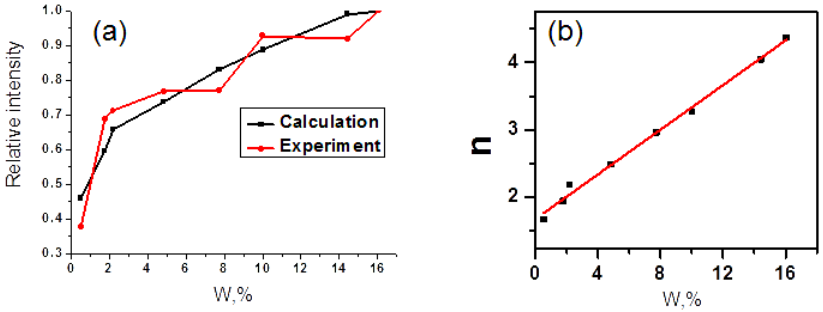

Fig. 6. Relative intensity of the signal reflected from the upper boundary (a) and dependence of absolute refraction index of river sand on moisture (b).

Figure 7a also demonstrates the results of experimental data processing. Comparison of theoretical and experimental data allows estimating relative deviation to be 0.10 – 0.15%.

The problem of establishing the correlation between the value of dielectric permittivity and the water content in soil samples is addressed in [25]. It is shown in this paper that this dependence can be approximated with the inaccuracy less than 10% by a third-degree polynomial:

$$\varepsilon = A + BW + CW^2 + DW^3 \tag{13}$$

where the parameters A, B, C and D depend on the composition of a sample, but approximately related as: 1:9:60:30. It's obvious that the main contribution to the approximation of the dielectric permittivity is given by the quadratic term. Since $n \sim \sqrt{\varepsilon}$, one can suppose that correlation between the value of absolute index of refraction and the

water content (moisture *W*) should be close to linear. This correlation obtained in this work for fine river sand is shown in Figure 6b.

4 Conclusions

In this work, a method is proposed to determine the complex dielectric permittivity and moisture of ground layers using the GPR technique calibrated with laboratory measurements of respective quantities. The method combines the advantages of a high-speed GPR method with a limited number of calibration measurements with a laborious laboratory resonance method of measuring the complex permittivity at frequencies commonly used in the practice of GPR. It provides determination of permittivity and conductivity of structural layers with an error not exceeding 10-15%. This makes it promising for use in software complexes for automatic processing of the GPR information in the monitoring of extended sections of roads and railways.

This work of G. Lazorenko is supported by the Russian Science Foundation under grant 17-79-10364 and performed in the Rostov State Transport University.

References

1. A. Annan, Subsurf. Sens. Technol. Appl. **3**, 253 (2002)
2. W. Wai-Lok Lai, X. Dérobert, P. Annan, NDT E Int. **96**, 58 (2018)
3. T. Saarenketo, J. Scullion, J. Appl. Geophys. **43**, 119 (2000)
4. Z. Khakiev, V. Bilalov, A. Morozov, V.Yavna, First break. **27**, 93 (2009)
5. L. Krysiński, J. Sudyka, Appl. Geophys. **97**, 27 (2013)
6. N. Diamanti, D. Redman, J. Appl. Geophys. **81**, 106 (2012)
7. M. Ahmed, R. Tarefder, A. Maji, Case Stud. Nondestr.Test. Eval. **6**, 94 (2016)
8. A. Benedetto, J. Appl. Geophys. **71**, 26 (2010)
9. A. Alani, M. Aboutalebi, G. Kilic, J. Appl. Geophys. **97**, 45 (2013)
10. H. Liu, M. Sato, NDT E Int. **64**, 65 (2014)
11. W.L. Lai, S.C. Kou, W.F. Tsang, C.S. Poon, Cem. Concr. Res. **39**, 687 (2009)
12. F. Tosti, C. Patriarca, E. Slob, A. Benedetto, S. Lambot, J. Appl. Geophys. **97**, 69 (2013)
13. J. Zhang, H. Lin, J. Doolittle, Geoderma. **213**, 560 (2014)
14. A. Kasprzhitskii, G. Lazorenko, V. Yavna, P. Daniel, J. Mol. Struct. **1109**, 97 (2016)
15. A. Kasprzhitskii, G. Lazorenko, A. Khater, V. Yavna, Minerals **8(5)**, 184 (2018)
16. B. Schmalz, B. Lennartz, J. Hydrol. **267(3-4)**, 217 (2002)
17. A. Benedetto, J. Appl. Geophys. **97**, 37 (2013)
18. Z. Khakiev, V. Shapovalov, A. Kruglikov, V. Yavna, J. Appl. Geophys. **106**, 139 (2014)
19. A. Kruglikov, V. Yavna, G. Lazorenko, Z. Khakiev, Proceedings of the 15th International Conference on Ground Penetrating Radar, **6970549** 857 (2014)
20. Y. Wang, H. Jin, G. Li, Cold. Reg. Sci. Technol. **126**, 10 (2016)
21. C. Yuan, S. Li, S. Li, W. Li, CJRME **30**, 3354 (2011)
22. J.H. Dane, G.C. Topp, *Methods of Soil Analysis* (SSSA Book Series, 2002)
23. Z. Khakiev, K. Kislitsa, V. Yavna, J. Appl. Geophys. **112(12)**, 124909 (2012)
24. M. Born, E. Wolf, *Principles of Optics* (Cambridge University Press, 1999)
25. G.C. Topp, J.L. Davis, A.P. Annan, Soil Sci. Soc. Am. J. **46**, 672 (1982)